Published in final edited form as:
J Immunol. 2010 July 15; 185(2): 1265–1273. doi:10.4049/jimmunol.0902808.

The Relative Timing of Exposure to Phagocytosable Particulates and to Osteoclastogenic Cytokines Is Critically Important in the Determination of Myeloid Cell Fate

Douglas E. James, **Bryan J. Nestor**, **Thomas P. Sculco**, **Lionel B. Ivashkiv**, **F. Patrick Ross**, **Steven R. Goldring**, and **P. Edward Purdue**
Hospital for Special Surgery, New York, NY 10021

Abstract

During granulomatous inflammatory reactions, myeloid cells can differentiate into activated phagocytic macrophages, wound-healing macrophages, foreign body giant cells, and bone-resorbing osteoclasts. Although it is appreciated that a variety of stimuli, including cytokines, cell–matrix interactions, and challenge with foreign materials can influence myeloid cell fate, little is known of how these signals integrate during this process. In this study, we have investigated the cross talk between receptor activator of NF-κB ligand (RANKL)-induced osteoclastogenesis and particle phagocytosis-induced activation of human monocytes. Understanding interconnected signals is of particular importance to disorders, such as periprosthetic osteolysis, in which granulomatous inflammation is initiated by particle phagocytosis in proximity to bone and leads to inflammatory bone loss. Using cell-based osteoclastogenesis and phagocytosis assays together with expression analysis of key regulators of osteoclastogenesis, we show in this study that phagocytosis of disease-relevant particles inhibits RANKL-mediated osteoclastogenesis of human monocytes. Mechanistically, phagocytosis mediates this effect by downregulation of RANK and c-Fms, the receptors for the essential osteoclastogenic cytokines RANKL and M-CSF. RANKL pretreatment of monocytes generates preosteoclasts that are resistant to RANK downregulation and committed to osteoclast formation, even though they retain phagocytic activity. Thus, the relative timing of exposure to phagocytosable particulates and to osteoclastogenic cytokines is critically important in the determination of myeloid cell fate.

Osteoclasts, multinucleated foreign body giant cells, and mononuclear phagocytic macrophages are derived from a common myeloid precursor (1,2). Multiple factors control the commitment of these precursors to each of the cell types, including cytokines, cell–cell, and cell–matrix interactions, but the details of when and where these cell fate determinations are made remain the subject of controversy. It has been established that differentiation of the common monocytic precursor toward osteoclasts is triggered by the presence of two key cytokines, MCSF and receptor activator of NF-κB ligand (RANKL), which signal through the myeloid receptors c-Fms and RANK, respectively (1,3). Signals associated with myeloid cell activation, such as stimulation of TLRs or IFN signaling, preferentially direct cell fate away from osteoclastogenesis, although many of the details responsible for this outcome are not well understood (4–8). The interplay of pro- and antiosteoclastogenic signaling is highly relevant to skeletal disorders, such as rheumatoid arthritis and related forms of inflammatory

Address correspondence and reprint requests to Dr. P. Edward Purdue, Hospital for Special Surgery, 535 East 70th Street, New York, NY 10021. purduee@hss.edu.

Disclosures
The authors have no financial conflicts of interest.

arthritis, in which myeloid precursors are exposed to potentially competing cell fate determination signals.

Phagocytosis represents an additional important pathway of myeloid cell activation (9), and phagocytosis of nondegradable materials is a common feature of a number of human diseases including silicosis, asbestosis, and the inflammatory reaction associated with orthopedic implant wear debris (10,11). In these disorders, activation of the phagocytic cells by particle uptake represents a key factor in the pathogenesis of tissue damage and organ dysfunction. What is less clear is how phagocytosis of particulate material influences the eventual cell fate determination of these cells.

The foreign body reaction associated with orthopedic wear particles released from orthopedic implant prostheses represents a particularly useful model for investigating the influence of phagocytosis on myeloid cell differentiation. Released wear particles induce a granulomatous inflammatory reaction associated with cells expressing phenotypic features of activated macrophages and macrophage polykaryons (10). Multiple myeloid cell receptors are involved in interaction with wear debris particles, including complement receptor CR3 (polymethylmethacrylate [PMMA] particles) and scavenger receptors (titanium particles) (12). Of importance, in regions where myeloid cell precursors are in direct contact with the bone surface, these precursors differentiate into activated osteoclasts that are responsible for local osteolysis. The effects of phagocytosis on osteoclast differentiation are conflicting. It has been reported that particles of PMMA can induce osteoclastogenesis in murine bone marrow macrophages pre-exposed to RANKL for 3 d, suggesting that phagocytosis may promote osteoclast formation (13,14). In contrast, particles are not clearly evident within osteoclasts in tissues retrieved from osteolysis patients, whereas activated macrophages in such tissues contain abundant particles (10,15). In this paper, we address the interplay between RANKL-induced osteoclastogenesis and phagocytic cell activation and provide mechanistic insights into how the balance and timing of these stimuli determine myeloid cell fate. In particular, we show that phagocytic activation of myeloid cells strongly represses expression of cell-surface receptors required for osteoclast formation, thus blocking these cells from becoming functional osteoclasts.

Materials and Methods

Cell culture

CD14-positive monocytes were prepared from PBMCs derived from deidentified normal human donors as described previously (16). Cells were then cultured at a cell density of 1–2 × 10^6 cells/ml in α-MEM medium (Invitrogen, Carlsbad, CA) supplemented with 10% FBS (VWR, West Chester, PA) and 1% antibiotic/antimycotic (Invitrogen) in the presence or absence of 25 ng/ml human M-CSF (PeproTech, Rocky Hill, NJ) in 12-well tissue-culture plates (1 ml/well). For osteoclastogenesis, cell density was reduced to 2.5 × 10^5 cells/ml, and 40 ng/ml human soluble RANKL (PeproTech) was included in the medium. Where indicated, MAPK and metalloprotease inhibitors were added 30 min prior to other treatments. The inhibitors used were SB203580 (p38, 10 μM), U0126 (MEK, 20 μM), SP600125 (JNK, 20 μM), and InSolution TNF-α protease inhibitor (TAPI) (TACE, 50 μM) from Calbiochem (San Diego, CA). For fluorescence microscopy, sterile glass coverslips were included in the wells prior to addition of cells. Where noted, human TNF-α or IFN-γ (PeproTech) or *Escherichia coli* LPS (Sigma-Aldrich, St. Louis, MO) were included in the cultures. Particles of PMMA, titanium, and silica were prepared and added as detailed below. Osteoclastogenesis was monitored by observation under light microscopy prior to processing for tartrate-resistant acid phosphatase (TRAP) staining, fluorescence microscopy, or RNA extraction.

Particles

PMMA particles (catalog number 19130, Polysciences, Warrington, PA; average diameter 6.06 μm), and commercially pure titanium (catalog number 00681, Johnson Matthey, Ward Hill, MA; average diameter 4.86 μm) were prepared and sterilized as described previously (16). Fluorescent green silica particles (catalog number PSi-G4.0; diameter 4 μm, 50 mg/ml) were from G. Kisker, Steinfurt, Germany). Only endotoxin-free particles as determined by *Limulus* assay (E-toxate, Sigma-Aldrich) were used in this study.

RNA extraction real-time quantitative RT-PCR

RNA was extracted (RNeasy Mini kit, Qiagen, Valencia, CA) and assessed for concentration and purity by OD measurement. A total of 500 ng aliquots of total cellular RNA were reversely transcribed using oligo(dT) primers and Moloney murine leukemia virus reverse transcriptase (First Strand cDNA Synthesis Kit, Fermentas, Burlington, Ontario, Canada) as recommended by the manufacturer. Real-time quantitative PCR (qPCR) was carried out in duplicate using the iCycler iQ thermal cycler detection system (Bio-Rad, Hercules, CA). Reactions included iQ SYBR Green Supermix reagent (Bio-Rad), 10 ng cDNA, and forward and reverse primers each at a concentration of 250 nM in a total volume of 25 μl. mRNA amounts were normalized relative to the housekeeping genes HPRT or GAPDH. Generation of only the correct amplification products was confirmed using melting point curve analysis of the products. The sequences of the oligonucleotide primers used were: human hypoxanthine phosphoribosyltransferase sense: 5′-TGAGGATTTGGAAAGGGTG-3′ and antisense: 5′-GAGGGCTACAATGTGATGG-3′; human GAPDH sense: 5′-ATCAAGAAGGTGGTGAAGCA-3′ and antisense: 5′-GTCGCTGTTGAAGTCAGAGGA-3′; human cathepsin K sense: 5′-TGAGGCTTCTCTTGGTGTCCATAC-3′ and antisense: 5′-AAAGGGTGTCATTACTGCGGG-3′; human Annexin VIII sense: 5′-AAAGGTGCCCCCGAGGTGA-3′ and antisense: 5′-GCCGCTGCGTGTTGCTTCT-3′; human RANK sense: 5′-CCTTGCCTTGCAGGCTACTT-3′ and antisense: 5′-TGGTGGTTTTCTAGCTGGCAG-3′; human c-Fms sense: 5′-GTGGCTGTGAAGATGCTGAA-3′ and antisense: 5′-CCCAGAAGGTTGACGATGTT-3′; human dendritic cell-specific transmembrane protein (DC-STAMP) sense: 5′-AAAGCTTGCCAGGGTTTGAG-3′and antisense: 5′-GGTTTTGGGATACAGTTGGGTTC-3′; and human ATP6v0d2 sense: 5′-AACGTAGCGGATCATTACGG-3′ and antisense: 5′-CACTGCCACCTACAGCTTCA-3′.

Immunoblot analysis

Protein extracts were prepared by SDS gel electrophoresis sample buffer, separated on 10% SDS-polyacrylamide gels (Bio-Rad), and transferred to polyvinylidene difluoride membranes (Millipore, Billerica, MA) by wet or semidry transfer. Membranes were incubated with specific Abs for c-Fms (#ab37858, Abcam, Cambridge, MA), IκBα, p-IκBα, phospho-p38 (#4814, #9246, and #9215, Cell Signaling Technology, Beverly, MA), and β-actin (A5316, Sigma-Aldrich). Membranes were subsequently incubated with anti-rabbit IgG or anti-mouse IgG, HRP-linked secondary Abs (#7076 and #7074, Cell Signaling Technology). Detection was with ECL or ECL Plus (GE Healthcare, Buckinghamshire, U.K.). Relative intensity levels were determined using ImageJ Freeware (National Institutes of Health, Bethesda, MD).

c-Fms ectodomain ELISA

Conditioned medium was collected and analyzed using an ELISA kit for c-Fms (DY329, R&D Systems, Minneapolis, MN) in accordance with the manufacturer’s protocol.

Fluorescence microscopy

Aliquots of 15×10^6 CD14-positive monocytes were incubated in tissue-culture plastic dishes for 24 h at 1.5×10^6 cells/ml in α-MEM medium supplemented with 25 ng/ml human M-CSF in the presence or absence of PMMA (20 particles/cell). This incubation allowed for complete phagocytosis of the added particles. Cells were then collected by flushing in cold PBS and washed in HBSS (Invitrogen). Aliquots of 5×10^6 cells with or without phagocytosed PMMA were then labeled with PKH2 Red Fluorescent Cell Linker Kit for Phagocytic Cell Labeling or PKH2 Green Fluorescent Cell Linker Kit for Phagocytic Cell Labeling (Sigma-Aldrich), respectively, in accordance with the manufacturer's recommendations. A concentration of 10 μm PKH dye/ml diluent was found to be sufficient for efficient cell labeling without deleterious effects on cell viability or subsequent osteoclastogenesis. Following fluorescent labeling, the cell populations were incubated for a further 24–48 h in α-MEM medium supplemented with 25 ng/ml human M-CSF. Finally, cells were plated on coverslips for osteoclastogenesis assays (see above). For the osteoclastogenic assays, the cell populations lacking PMMA (labeled green) or containing PMMA (labeled red) were incubated separately or in combinations of 1:1, 1:3, and 3:1 at 2.5×10^5 cells/well.

For labeling with fluorescent silica particles, aliquots of 15×10^6 CD14-positive monocytes were incubated on tissue-culture plastic dishes for 24 h at a density of 1.5×10^6 cells/ml in α-MEM medium supplemented with 25 ng/ml human M-CSF in the presence or absence of fluorescent green silica particles (33–66 pg/cell) and then collected by flushing with cold PBS. Cells lacking particles were labeled with PKH2 Red Fluorescent Cell Linker Kit for Phagocytic Cell Labeling (Sigma-Aldrich). Subsequent steps culminating in osteoclastogenesis assays were as described for the experiments with PMMA. After 7–9 d following addition of RANKL, the coverslips were mounted onto slides in Vectastain mounting medium containing DAPI (Vector Laboratories, Burlingame, CA) and photographed. Phalloidin red staining was carried out using Texas Red-X phalloidin (Invitrogen) according to manufacturer's recommendations. Quantitation of silica particles per nucleus in osteoclasts was calculated by counting nuclei and particles in 20 cells with three or more nuclei.

TRAP staining

A staining kit for TRAP was obtained from Sigma-Aldrich and used in accordance with the manufacturer's recommendations. For quantitation of osteoclastogenesis, entire wells were counted for TRAP-positive cells containing three or more nuclei.

Results

Phagocytosis inhibits RANKL-induced osteoclastogenesis

In the presence of 40 ng/ml RANKL, human monocytes underwent osteoclastogenesis as evidenced by the formation of multinucleated TRAP-positive cells. No significant multinucleation or TRAP expression was observed in the absence of RANKL. When titanium or PMMA particles were included in the cultures at a particle to cell ratio of 20:1, the cells efficiently phagocytosed the particles but failed to form multinucleated osteoclasts. Complete inhibition of osteoclastogenesis was also seen in the presence of 10 U/ml IFN-γ, with a partial inhibition seen at a dose of 1.5 U/ml (Fig. 1*A*). Inhibition of osteoclastogenesis by particle phagocytosis was dose dependent, with doses of 5–15 particles/cell resulting in partial, although significant, inhibition, whereas doses of 20–30 particles/cell resulted in complete repression of osteoclastogenesis (Fig. 1*B* and data not shown). These findings were supported by qPCR, which showed that particle phagocytosis strongly repressed

RANKL-induced expression of mRNA encoding the osteoclast markers cathepsin K and Annexin VIII (17) (Fig. 1*C*).

RANKL pretreatment inhibits the repressive effects of particle phagocytosis on osteoclastogenesis

In the above experiments, cells were exposed to phagocytosable particles and RANKL at the same time. Next, we evaluated the effects of particle phagocytosis on cells that had been pretreated with RANKL. Pretreatment with RANKL for as little as 24 h blocked the ability of PMMA or titanium (but not IFN-γ) to downregulate osteoclastogenesis, whereas 3 d of RANKL pretreatment blocked the antiosteoclastogenic effects of both phagocytosis and IFN-γ (Fig. 2*A*). This result was confirmed by qPCR analysis of cathepsin K and Annexin VIII mRNA expression (Fig. 2*B*). Significantly, the antiosteoclastogenic consequences of particle phagocytosis and repression of this by RANKL pretreatment were also seen with silica particles. RANKL-mediated osteoclasto-genesis was also suppressed effectively by phagocytosis of green fluorescent silica particles added concomitantly with RANKL, but not when the silica was added subsequent to a 2-d pretreatment with RANKL (Fig. 3*A*, *left panels*). These findings demonstrate that the observed antiosteoclastogenic effects are not restricted to orthopedic wear particles, but rather relate to a general effect of phagocytosis on myeloid cell commitment.

Cells committed toward osteoclast differentiation by RANKL retain phagocytic activity

When cells were pretreated with RANKL for 48 h prior to addition of PMMA, osteoclast formation was not only resistant to inhibition by particles, but was also accompanied by their efficient phagocytosis (Fig. 3*B*, *right panels*). Similar results were obtained using silica particles (Fig. 3*A*, *left panels*). These results suggest that RANKL pretreatment commits cells to osteoclast differentiation without repressing phagocytosis. In contrast, when silica or PMMA were added concomitantly with RANKL, but at reduced doses insufficient to completely repress osteoclastogenesis, the osteoclasts that formed contained few particles, whereas the cells that remained mononuclear contained large numbers of particles (Fig. 3*A*, *right panels* [silica], 3*B*, *left panels* [PMMA]). Quantitation revealed an ~8-fold increase in phagocytosed particles per nucleus in osteoclasts in response to RANKL pretreatment. Taken together, these results suggest that phagocytosis of significant numbers of particles strongly inhibits osteoclast formation from monocytes and that RANKL pretreatment represses this effect without repressing phagocytosis per se.

Particle-loaded cells are deficient in initiation of osteoclastogenesis, but incorporate into differentiating osteoclasts

The preceding results demonstrate that particle phagocytosis effectively inhibits the initiation of osteoclastogenesis in cells not previously exposed to RANKL. To address whether particle phagocytosis also affects the cell-fusion events that characterize the later stages of osteoclast formation, osteoclastogenesis assays were performed using mixtures of cells with or without phagocytosed particles. Fluorescence microscopy was employed to monitor the fates of both particle-free and particle-laden cells during osteoclastogenic assays. Two approaches were taken. First, the cytosol of cells lacking particles was labeled green, and the cytosol of cells bearing PMMA particles was labeled red. As expected, cells lacking particles underwent RANKL-mediated osteoclastogenesis, whereas cells containing particles failed to multinucleate in the presence of RANKL (Fig. 4*A*). When the two cell populations were cocultured in equal quantities with RANKL, osteoclasts with two distinct patterns of fluorescence were detected, characterized by either green but no red fluorescence, representing osteoclasts formed through complete exclusion of cells that has phagocytosed PMMA particles or by both red and green fluorescence, representing osteoclasts formed from cells with and without particles (Fig. 4*B*). No osteoclasts displaying

red but not green fluorescence were observed, confirming that particle-bearing cells cannot initiate osteoclastogenesis. These findings suggest that despite being unable to initiate osteoclast formation, particle-bearing cells may incorporate into polykaryons during subsequent stages of differentiation. In support of this assertion, monocyte expression of DC-STAMP and ATP6v0d2, proteins closely involved with cell-fusion events during osteoclastogenesis, were induced following phagocytosis (Fig. 4*C*).

In a second approach, cells loaded with green fluorescent silica particles were incubated alone or in the presence of particle-free cells that had been cytoplasmically labeled red. In accordance with the results with PMMA, particle-bearing cells were unable to initiate osteoclastogenesis (Fig. 5*A*). Through the use of phalloidin labeling of the osteoclast actin ring, it was further observed that, although generally being excluded from the multinuclear cells, silica particles were present to a limited extent (Fig. 5*B*, 5*C*), suggesting that, as seen for PMMA-loaded cells, silica-loaded cells may participate to a limited degree in cell-fusion events during osteoclastogenesis, but are themselves unable to initiate an osteoclast differentiation program. To estimate the relative contributions of particle-free and particle-laden cells to the formation of osteoclasts, particles and nuclei were counted in silica-containing cells before and after osteoclastogenesis. Following phagocytosis, an average of 2.2 particles/nucleus were observed. Following osteoclastogenesis with an equal number of particle-free cells, a total of 29 osteoclasts contained 518 nuclei and 108 particles, a ratio of 0.21 particles/nucleus. Thus, the particle/nucleus ratio in the osteoclasts is ~10-fold lower than in the mononuclear phagocytes (0.21 compared with 2.2). This suggests that of the cells contributing to osteoclast formation, only ~10% contained particles, whereas 90% were particle-free.

Particle phagocytosis represses expression of RANK and c-Fms, the key receptors for osteoclastogenesis

To investigate the mechanisms by which phagocytosis inhibits osteoclastogenesis, gene expression patterns in cells treated with or without particles were analyzed by qPCR. Notably, RANK mRNA was repressed strongly following phagocytosis. RANK expression is low in freshly isolated monocytes and induced by M-CSF treatment (Fig. 6*A*). Phagocytosis both inhibited this M-CSF–dependent induction of RANK mRNA (Fig. 6*A*) and also repressed RANK expression in M-CSF–pretreated cells (Fig. 6*B*). Repression of RANK mRNA was evident 1 d following phagocytosis and was sustained at day 8 of cell culture (Fig. 6*B*). Particle phagocytosis-mediated inhibition of RANK expression was dose dependent (Fig. 6*C*), mirroring the dose dependency of particle-mediated repression of osteoclastogenesis (Fig. 1*B*). Although phagocytosis-mediated repression of RANK was still evident in the presence of RANKL, RANKL pretreatment diminished the repressive effects of phagocytosis on RANK expression, consistent with the observation that RANKL pretreatment diminishes the antiosteoclastogenic effects of particle phagocytosis (Fig. 6*D*). Interestingly, RANKL itself also resulted in a modest decrease in RANK expression (Fig. 6*D*). To investigate the possible mechanism of RANK repression, cells were treated with MAPK inhibitors prior to particle treatment. Inhibition of MEK, but not p38 or JNK MAPKs, prevented the repression of RANK induced by phagocytosis (Fig. 6*E*). To investigate the functional consequences of phagocytosis-mediated repression of RANK, monocytes were cultured for 24 h with or without particles prior to addition of RANKL. Consistent with loss of RANK, particle-laden cells demonstrated a reduced ability to phosphorylate p38 and IκBα in response to RANKL (Fig. 6*F*, 6*G*).

In addition to RANKL signaling through RANK, osteoclastogenesis is also dependent on the presence of M-CSF, which signals through its receptor, c-Fms (3). Similar to its effect on the repression of RANK, phagocytosis of particles resulted in strong downregulation by 24 h after particle addition of both c-Fms mRNA (Fig. 7*A*) and protein (Fig. 7*C*). Phagocytosis-

mediated repression of c-Fms mRNA was particle dose dependent (Fig. 7*B*). c-Fms protein was markedly repressed at 3 and 24 h postinitiation of phagocytosis, but not at 1 h. This contrasts with LPS-mediated depletion of c-Fms, which is complete within 1 h (Fig. 7*C*). Phagocytosis-mediated c-Fms downregulation was dependent upon ERK and JNK activities, being inhibited by U0216 and SP600125, but only modestly by the p38 MAPK inhibitor SB203580 (Fig. 7*D*). Furthermore, the metalloprotease inhibitor TAPI prevented loss of c-Fms expression in response to silica or PMMA particle phagocytosis, implicating involvement of metalloprotease-mediated receptor shedding in c-Fms downregulation following phagocytosis (Fig. 7*E*). This was supported by the observation that shed c-Fms ectodomain in the conditioned media of cells was sharply increased after PMMA phagocytosis by a TAPI-sensitive mechanism (Fig. 7*F*).

TNF and IFN-α/β are not involved in phagocytosis-mediated inhibition of osteoclastogenesis

TNF has been reported to act as a pro-osteoclastogenic cytokine, either through synergistic action with RANKL or possibly through an alternative RANKL-independent pathway (18,19). Because TNF does not signal via RANK (which is downregulated by particle phagocytosis), we investigated whether TNF was able to rescue osteoclastogenesis in the presence of particles. Although synergism with low doses of RANKL was observed, TNF alone showed no pro-osteoclastogenic activity within the 7–9 d time frame of RANKL-induced osteoclastogenesis used in this study. However, in no case was the repressive effect of PMMA phagocytosis on RANKL-mediated osteoclastogenesis modified by the presence of TNF at any dose. In addition, blockade of TNF with etanercept had no discernable effect on phagocytosis-mediated inhibition of osteoclast formation (data not shown). In addition, expression of IFN-β, a known negative regulator of osteoclastogenesis (20), was not modulated by particle phagocytosis, and blocking IFN-α/β signaling with blocking Abs to the IFN-α/β receptor had no observable effects on phagocytosis inhibition of osteoclastogenesis (data not shown).

In summary, we have shown that particle phagocytosis inhibits RANKL-induced osteoclastogenesis by downregulating RANK and c-Fms expression and that RANKL pretreatment commits cells to osteoclastogenesis by inhibiting these effects of particle phagocytosis while not inhibiting phagocytosis per se.

Discussion

We have shown in this study that phagocytosis of nondegradable particulate matter, including the orthopedic wear components PMMA, titanium, and silica, can inhibit RANKL-mediated osteoclastogenesis. Of importance, the antiosteoclastogenic effects of phagocytosis of PMMA, titanium, or silica can be effectively reversed by pre-exposure of the cells to RANKL prior to particle addition. This finding suggests that RANKL is able to provide an osteoclast commitment signal that overrides subsequent particle effects that normally result in granuloma formation. The ability to generate osteoclasts does not manifest as downregulation of phagocytic potential, because the RANKL-pretreated cells maintain a high capacity for particle ingestion, a finding consistent with studies showing that murine macrophages committed to osteoclastogenesis by RANKL treatment maintain the ability to phagocytose zymosan particles (21).

Various stimuli, including TLR stimulation, zymosan particles, and antiosteoclastogenic cytokines IL-4 and IFN-γ, have previously been shown to share the ability to repress RANKL-mediated osteoclast formation (4–8,21–23). Mechanistically, it has been proposed that IFN-γ inhibits osteoclastogenesis through stimulation of proteasomal degradation of TRAF6, whereas LPS binding to TLR4 decreases expression of c-Fms and RANK, the

receptors for the osteoclastogenic cytokines M-CSF and RANKL. Recent reports have suggested that LPS or stimulation of TLR5 inhibits osteoclastogenic differentiation via STAT1-dependent induction of IFN-β (4). Our studies were designed to determine to what extent the antiosteoclastogenic effects of phagocytic cell activation use these known mechanisms of diverting myeloid cell differentiation away from commitment to the osteoclast differentiation pathway. Our results strongly implicate a mechanism that involves potent downregulation of both RANK and c-Fms expression and thus indicate a shared mechanism for the antiosteoclastogenic effects of particle phagocytosis and TLR pathway activation. By contrast, phagocytosis did not induce IFN-β expression, and particle-mediated repression of osteoclastogenesis was not modulated by inhibiting IFN-α or -β signaling with blocking Abs.

In our studies, we found that repression of M-CSF–induced RANK expression by phagocytosis was rapid and long lasting. Inhibitor studies implicated involvement of ERK, but not p38 or JNK MAPKs in the particle phagocytosis-mediated repression of RANK mRNA expression. Downregulation of RANK was reflected by the failure of RANKL to initiate signaling pathways, such as phosphorylation of IκBα and p38 in particle-laden cells. RANKL pretreatment made cells refractory to phagocytosis-mediated downregulation of RANK, consistent with the ability of RANKL pretreatment to reverse the antiosteoclastogenic effects of particle phagocytosis. Taken together, these results suggest that downregulation of RANK expression may represent an important mechanism for the antiosteoclastogenic effects of particle phagocytosis. Concomitant with RANK repression, and in common with LPS stimulation via TLR4 (8) and IL-4 signaling (24), phagocytosis also resulted in potent loss of expression of c-Fms, the receptor for MCSF. These data suggest that the decrease in RANK and c-Fms expression induced by phagocytosis was dependent on several different mechanisms involving both receptor shedding and receptor synthesis. Involvement of receptor shedding in phagocytosis-mediated repression of c-Fms was verified by appearance of the shed ectodomain of this receptor in the conditioned medium, an event blocked by pretreatment with TAPI, a general inhibitor of hydroxamic acid-base-metalloproteinase and a disintegrin and metalloprotease proteins, which have been implicated in the shedding of several different cell-surface receptors (25). In addition to receptor shedding, our results indicate that receptor synthesis is also affected by phagocytosis. We have previously shown rapid activation of p38, MEK/ERK, and JNK MAPKs in response to particle phagocytosis (16). Our results implicate all three of these classes of activated MAPKs, but most prominently MEK/ERK and JNK, in c-Fms downregulation. The rapid, comprehensive downregulation of RANK and c-Fms by phagocytosis provides a compelling mechanistic explanation for the antiosteoclastogenic effects of this pathway of myeloid cell activation.

Although cells that have phagocytosed particles are unable to initiate RANKL-mediated osteoclastogenesis, they were underrepresented but not totally excluded in osteoclasts formed in coculture with particle-free cells. This suggests that phagocytosis does not prevent participation in the later cell fusion events responsible for the formation of multinucleated osteoclasts. Our findings that particle phagocytosis induces expression of DC-STAMP and ATP-6v0d2, two proteins involved in cell fusion during osteoclastogenesis (26,27), provide a possible explanation for the ability of phagocytic cells to participate in the process of osteoclast multinucleation events during in vitro coculture. In this regard, it is of interest to note that both DC-STAMP and ATP6v0d2 are regulated by NFATc1, a key transcription factor for osteoclastogenesis (28), and it has recently been reported that phagocytosis of PMMA particles activated NFATc1 in murine bone marrow-derived macrophages (14).

The influences of particle phagocytosis on osteoclastogenesis (and vice versa) are of especial importance to an understanding of the cellular basis of periprosthetic osteolysis, in

which macrophage lineage cells coexist in an environment rich in both phagocytosable particles and osteoclastogenic cytokines. In our previous studies, we showed that the phenotype of cells present with the granuloma was markedly affected by the substrate with which the cells interacted. We observed that cells attached to the polymeric wear particles expressed some, but not all, of the phenotypic markers of osteoclasts, although the levels of the osteoclast-associated genes were considerably lower compared with the multinucleated osteoclasts in resorption lacunae on the bone surfaces (29–31). Both the multinucleated and mononuclear cells within the granuloma contained abundant phagocytosed wear particles. In contrast, the osteoclasts on the bone surfaces tended to be devoid of particles. These findings recapitulate the observations of Willert et al. (15), who noted that osteoclasts within the osteolytic tissues associated with periprosthetic osteolysis did not appear to contain particles. We have also recently shown that a subset of mononuclear cells present in peri-implant granuloma associated with particulate prosthetic wear debris express phenotypic features of macrophages that exhibit an alternative activation phenotype with similarities to that observed in the cells of patients with lysosomal storage diseases, such as Gaucher disease (32). These results suggest that, in addition to the acute short-term effects of particle internalization, the continued presence of particles in the phagocytes influences the pattern of gene expression and phenotype of macrophages. Overall, these in vivo observations provide support for our in vitro studies indicating that myeloid lineage cells engaged in particle phagocytosis are diverted away from osteoclast differentiation.

Acknowledgments

This work was supported in part by an American College of Rheumatology-Research and Education Within Our Reach: Innovative Research Grant (to S.R.G.). This investigation was conducted in a facility constructed with support from Research Facilities Improvement Program Grant C06-RR12538-01 from the National Center for Research Resources, National Institutes of Health.

Abbreviations used in this paper

DC-STAMP	dendritic cell-specific transmembrane protein
PMMA	polymethylmethacrylate
qPCR	quantitative PCR
RANK	receptor activator of NF-κB
RANKL	receptor activator of NF-κB ligand
SB	SB203580
SP	SP600125
TAPI	TNF-α protease inhibitor
TRAP	tartrate-resistant acid phosphatase
U0	U0216

References

1. Boyle WJ, Simonet WS, Lacey DL. Osteoclast differentiation and activation. Nature. 2003; 423:337–342. [PubMed: 12748652]
2. Brodbeck WG, Anderson JM. Giant cell formation and function. Curr. Opin. Hematol. 2009; 16:53–57. [PubMed: 19057205]
3. Ross FP. M-CSF, c-Fms, and signaling in osteoclasts and their precursors. Ann. N. Y. Acad. Sci. 2006; 1068:110–116. [PubMed: 16831911]

4. Ha H, Lee JH, Kim HN, Kwak HB, Kim HM, Lee SE, Rhee JH, Kim HH, Lee ZH. Stimulation by TLR5 modulates osteoclast differentiation through STAT1/IFN-beta. J. Immunol. 2008; 180:1382–1389. [PubMed: 18209032]
5. Takami M, Kim N, Rho J, Choi Y. Stimulation by toll-like receptors inhibits osteoclast differentiation. J. Immunol. 2002; 169:1516–1523. [PubMed: 12133979]
6. Takayanagi H, Ogasawara K, Hida S, Chiba T, Murata S, Sato K, Takaoka A, Yokochi T, Oda H, Tanaka K, et al. T-cell-mediated regulation of osteoclastogenesis by signalling cross-talk between RANKL and IFN-gamma. Nature. 2000; 408:600–605. [PubMed: 11117749]
7. Zou W, Bar-Shavit Z. Dual modulation of osteoclast differentiation by lipopolysaccharide. J. Bone Miner. Res. 2002; 17:1211–1218. [PubMed: 12096834]
8. Ji J-D, Park-Min K-H, Shen Z, Fajardo RJ, Goldring SR, McHugh KP, Ivashkiv LB. Inhibition of RANK expression and osteoclastogenesis by TLRs and IFN-gamma in human osteoclast precursors. J. Immunol. 2009; 183:7223–7233. [PubMed: 19890054]
9. Aderem A. Phagocytosis and the inflammatory response. J. Infect. Dis. 2003; 187 Suppl 2:S340–S345. [PubMed: 12792849]
10. Purdue PE, Koulouvaris P, Potter HG, Nestor BJ, Sculco TP. The cellular and molecular biology of periprosthetic osteolysis. Clin. Orthop. Relat. Res. 2007; 454:251–261. [PubMed: 16980902]
11. Rimal B, Greenberg AK, Rom WN. Basic pathogenetic mechanisms in silicosis: current understanding. Curr. Opin. Pulm. Med. 2005; 11:169–173. [PubMed: 15699791]
12. Rakshit DS, Lim JT, Ly K, Ivashkiv LB, Nestor BJ, Sculco TP, Purdue PE. Involvement of complement receptor 3 (CR3) and scavenger receptor in macrophage responses to wear debris. J. Orthop. Res. 2006; 24:2036–2044. [PubMed: 16947312]
13. Clohisy JC, Frazier E, Hirayama T, Abu-Amer Y. RANKL is an essential cytokine mediator of polymethylmethacrylate particle-induced osteoclastogenesis. J. Orthop. Res. 2003; 21:202–212. [PubMed: 12568950]
14. Yamanaka Y, Abu-Amer W, Foglia D, Otero J, Clohisy JC, Abu-Amer Y. NFAT2 is an essential mediator of orthopedic particle-induced osteoclastogenesis. J. Orthop. Res. 2008; 26:1577–1584. [PubMed: 18655139]
15. Willert HG, Bertram H, Buchhorn GH. Osteolysis in alloarthroplasty of the hip. The role of bone cement fragmentation. Clin. Orthop. Relat. Res. 1990; (258):108–121. [PubMed: 2203567]
16. Rakshit DS, Ly K, Sengupta TK, Nestor BJ, Sculco TP, Ivashkiv LB, Purdue PE. Wear debris inhibition of anti-osteoclastogenic signaling by interleukin-6 and interferon-gamma. Mechanistic insights and implications for periprosthetic osteolysis. J. Bone Joint Surg. Am. 2006; 88:788–799. [PubMed: 16595469]
17. McHugh K, Shen Z, O'Sullivan R, Crotti T, Flannery M, Goldrin S. Annexin VIII Is a Critical Bone Matrix-dependent Osteoclast Gene Transcriptionally Regulated by RANKL and NFATc1. J. Bone Miner. Res. 2007; 22:S379.
18. Kudo O, Fujikawa Y, Itonaga I, Sabokbar A, Torisu T, Athanasou NA. Proinflammatory cytokine (TNFalpha/IL-1alpha) induction of human osteoclast formation. J. Pathol. 2002; 198:220–227. [PubMed: 12237882]
19. Lam J, Takeshita S, Barker JE, Kanagawa O, Ross FP, Teitelbaum SL. TNF-alpha induces osteoclastogenesis by direct stimulation of macrophages exposed to permissive levels of RANK ligand. J. Clin. Invest. 2000; 106:1481–1488. [PubMed: 11120755]
20. Takayanagi H, Kim S, Matsuo K, Suzuki H, Suzuki T, Sato K, Yokochi T, Oda H, Nakamura K, Ida N, et al. RANKL maintains bone homeostasis through c-Fos-dependent induction of interferon-beta. Nature. 2002; 416:744–749. [PubMed: 11961557]
21. Mochizuki A, Takami M, Kawawa T, Suzumoto R, Sasaki T, Shiba A, Tsukasaki H, Zhao B, Yasuhara R, Suzawa T, et al. Identification and characterization of the precursors committed to osteoclasts induced by TNF-related activation-induced cytokine/receptor activator of NF-kappa B ligand. J. Immunol. 2006; 177:4360–4368. [PubMed: 16982870]
22. Abu-Amer Y. IL-4 abrogates osteoclastogenesis through STAT6-dependent inhibition of NF-kappaB. J. Clin. Invest. 2001; 107:1375–1385. [PubMed: 11390419]

23. Moreno JL, Kaczmarek M, Keegan AD, Tondravi M. IL-4 suppresses osteoclast development and mature osteoclast function by a STAT6-dependent mechanism: irreversible inhibition of the differentiation program activated by RANKL. Blood. 2003; 102:1078–1086. [PubMed: 12689929]
24. Hiasa M, Abe M, Nakano A, Oda A, Amou H, Kido S, Takeuchi K, Kagawa K, Yata K, Hashimoto T, et al. GM-CSF and IL-4 induce dendritic cell differentiation and disrupt osteoclastogenesis through M-CSF receptor shedding by up-regulation of TNF-alpha converting enzyme (TACE). Blood. 2009; 114:4517–4526. [PubMed: 19762488]
25. Blobel CP. ADAMs: key components in EGFR signalling and development. Nat. Rev. Mol. Cell Biol. 2005; 6:32–43. [PubMed: 15688065]
26. Lee SH, Rho J, Jeong D, Sul JY, Kim T, Kim N, Kang JS, Miyamoto T, Suda T, Lee SK, et al. v-ATPase V0 subunit d2-deficient mice exhibit impaired osteoclast fusion and increased bone formation. Nat. Med. 2006; 12:1403–1409. [PubMed: 17128270]
27. Yagi M, Miyamoto T, Sawatani Y, Iwamoto K, Hosogane N, Fujita N, Morita K, Ninomiya K, Suzuki T, Miyamoto K, et al. DC-STAMP is essential for cell-cell fusion in osteoclasts and foreign body giant cells. J. Exp. Med. 2005; 202:345–351. [PubMed: 16061724]
28. Kim K, Lee SH, Ha Kim J, Choi Y, Kim N. NFATc1 induces osteoclast fusion via up-regulation of Atp6v0d2 and the dendritic cell-specific transmembrane protein (DC-STAMP). Mol. Endocrinol. 2008; 22:176–185. [PubMed: 17885208]
29. Shen Z, Crotti TN, McHugh KP, Matsuzaki K, Gravallese EM, Bierbaum BE, Goldring SR. The role played by cell-substrate interactions in the pathogenesis of osteoclast-mediated peri-implant osteolysis. Arthritis Res. Ther. 2006; 8:R70. [PubMed: 16613614]
30. Goldring SR, Roelke M, Glowacki J. Multinucleated cells elicited in response to implants of devitalized bone particles possess receptors for calcitonin. J. Bone Miner. Res. 1988; 3:117–120. [PubMed: 2850723]
31. Glowacki J, Jasty M, Goldring S. Comparison of multinucleated cells elicited in rats by particulate bone, polyethylene, or polymethylmethacrylate. J. Bone Miner. Res. 1986; 1:327–331. [PubMed: 3503546]
32. Koulouvaris P, Ly K, Ivashkiv LB, Bostrom MP, Nestor BJ, Sculco TP, Purdue PE. Expression profiling reveals alternative macrophage activation and impaired osteogenesis in periprosthetic osteolysis. J. Orthop. Res. 2008; 26:106–116. [PubMed: 17729302]

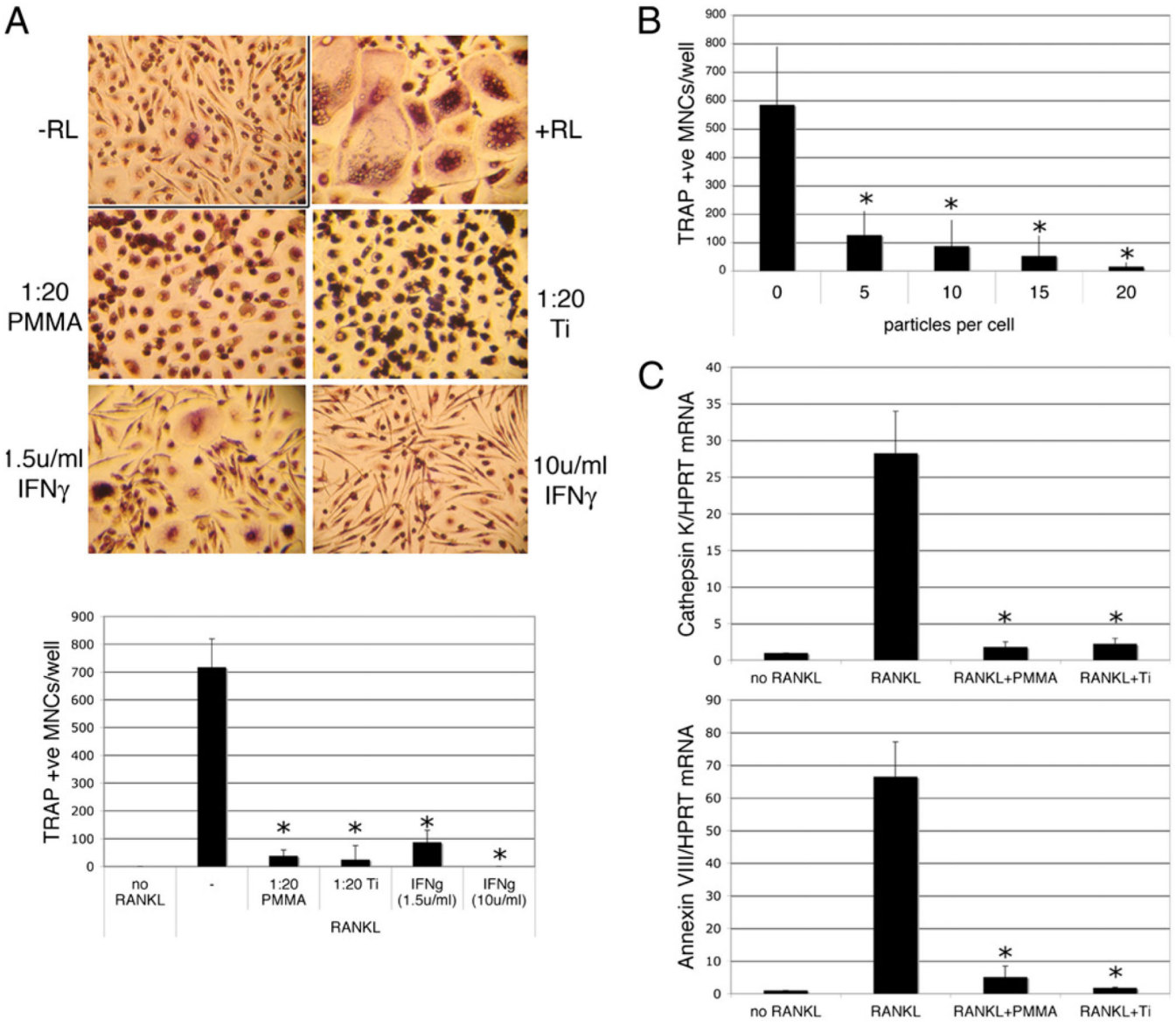

FIGURE 1.

Particle phagocytosis inhibits RANKL-mediated osteoclastogenesis. Preosteoclasts were cultured for 9 d in the presence of 25 ng/ml M-CSF in the presence or absence of RANKL (RL; 50 ng/ml). Particles of PMMA or titanium (Ti; 20 particles/cell) or IFN-γ (1.5 or 10 U/ml) were added at the same time as the RANKL. Following culture, cells were either stained for TRAP or processed for RNA extraction and qPCR. *A*, Representative images of TRAP-stained cells (original magnification ×50) and quantitation of TRAP-positive multinuclear (≥3 nuclei) cells. $n = 3$. *B*, Dose dependency of particle-mediated inhibition of RANKL-mediated osteoclastogenesis. $n = 3$. *C*, qPCR analysis of cathepsin K and Annexin VIII mRNA expression relative to GAPDH. $n = 4$. $^*p < 0.01$ compared with RANKL alone.

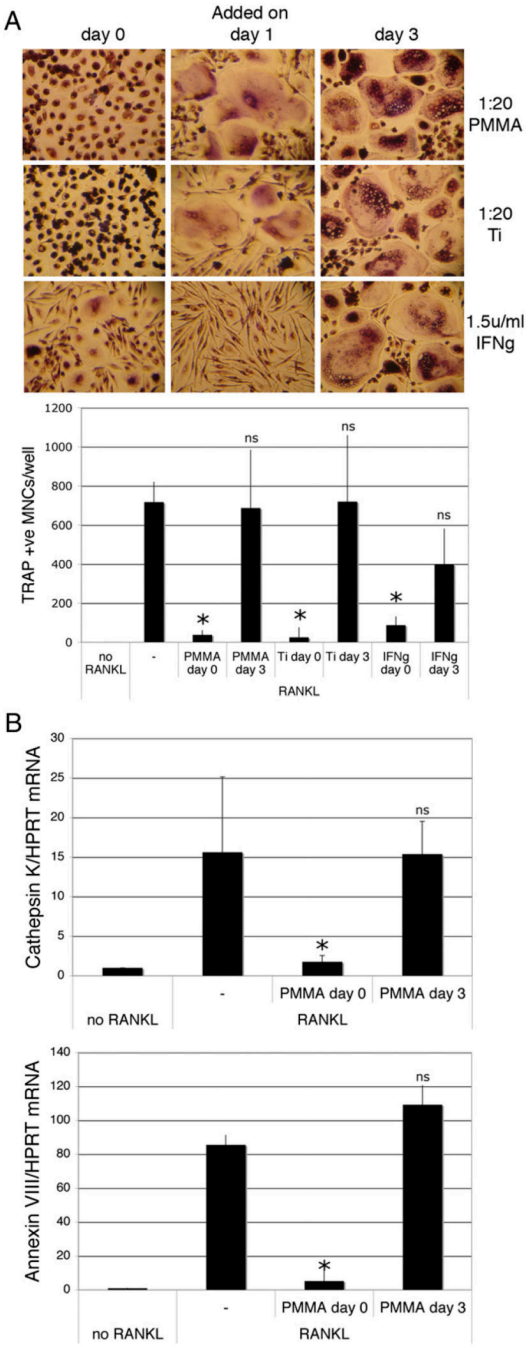

FIGURE 2.

RANKL pretreatment blunts particle phagocytosis-mediated inhibition of osteoclastogenesis. Preosteoclasts were cultured for 9 d in the presence of 25 ng/ml M-CSF and 50 ng/ml RANKL. Particles of PMMA or titanium (Ti; 20 particles/cell) or IFN-γ (1.5 U/ml) were added at the same time as the RANKL (day 0) or at various times after initial addition of RANKL. *A*, Representative TRAP staining of cells pretreated with RANKL for 0, 1, and 3 d and quantitation of TRAP-positive multinuclear cells (original magnification ×50). $n = 3$. *B*, qPCR for detection of cathepsin K and Annexin VIII mRNA of cells pretreated with RANKL for 0 and 3 d. $n = 4$. *$p < 0.01$ compared with RANKL alone.

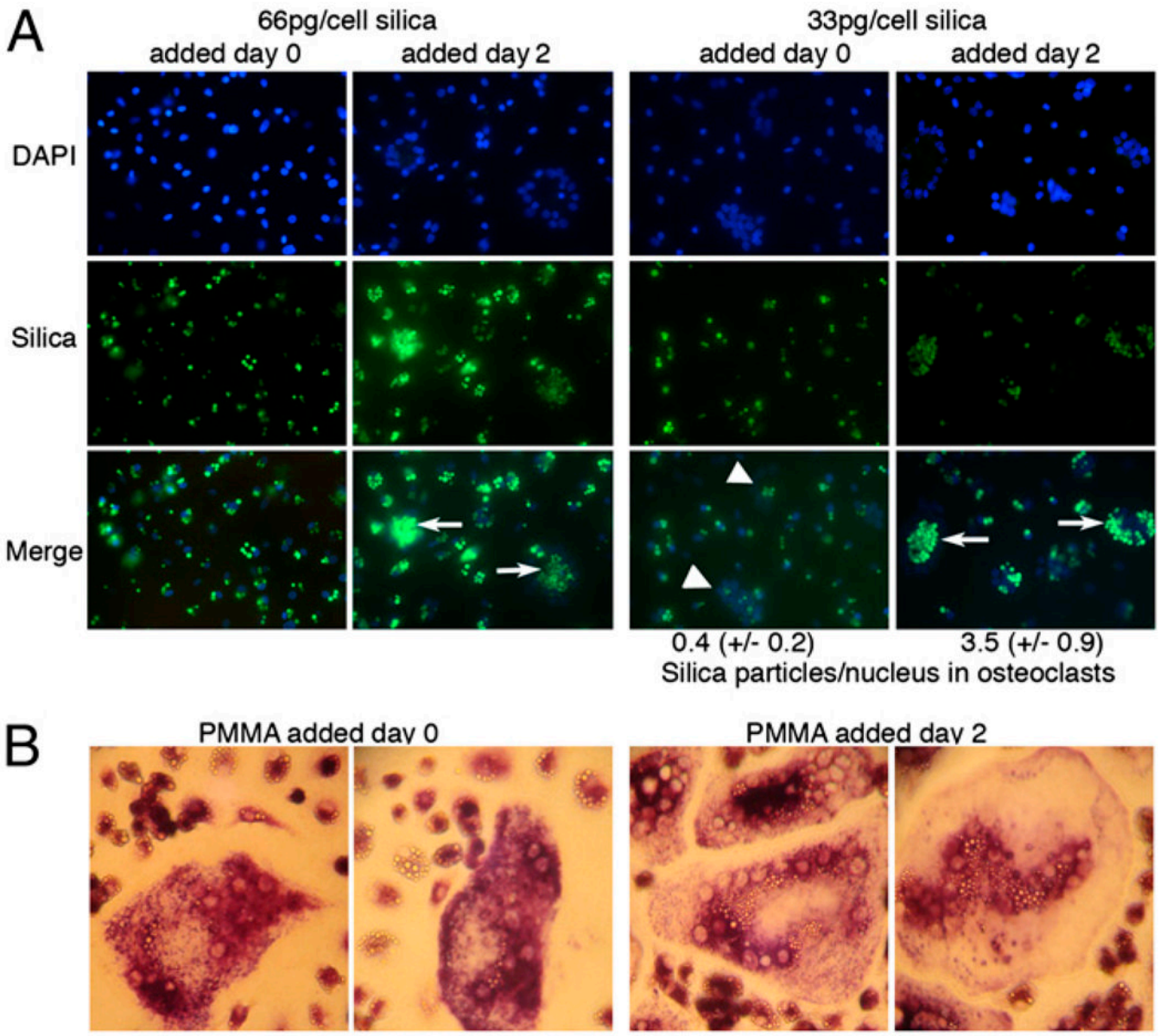

FIGURE 3.

RANKL-pretreated cells acquire both phagocytic and osteoclastogenic capacities. *A*, Preosteoclasts were cultured for 9 d in the presence of 25 ng/ml M-CSF and 50 ng/ml RANKL. Particles of green fluorescent silica were added at the same time as the RANKL (day 0) or 2 d after initial addition of RANKL. Cells were then analyzed by fluorescence microscopy (original magnification ×25). Arrows show osteoclasts formed in cells pretreated with RANKL; arrowheads show osteoclasts formed in cells without RANKL pretreatment. Particles per nucleus in osteoclasts were quantified as described in *Materials and Methods*. *B*, Preosteoclasts were cultured for 9 d in the presence of 25 ng/ml M-CSF and 50 ng/ml RANKL. Particles of PMMAwere added at the same time as the RANKL (day 0, 10 particles/cell) or 2 d after initial addition of RANKL (20 particles/cell). Osteoclastogenesis was determined by TRAP staining (original magnification ×100).

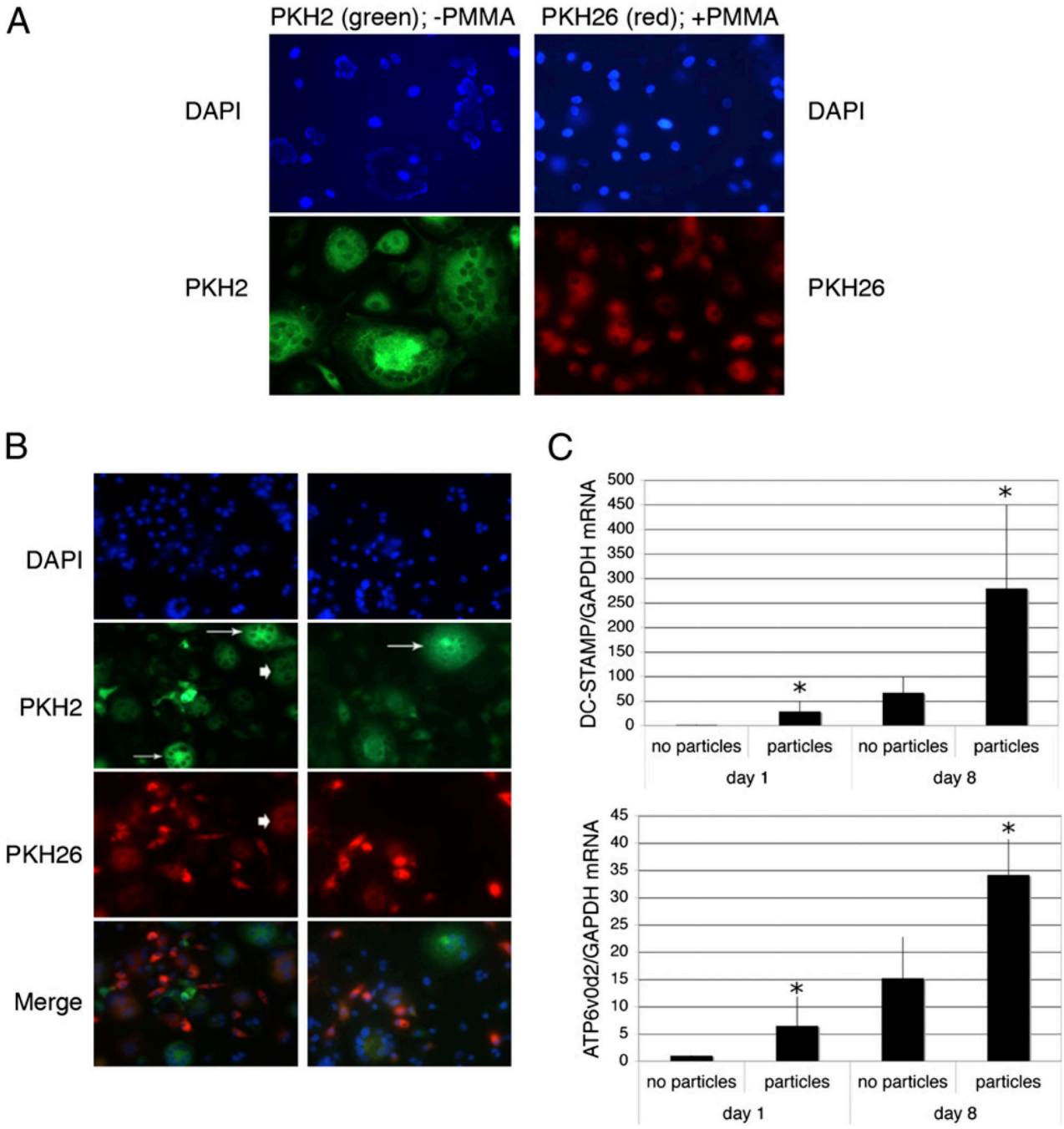

FIGURE 4.

Particle phagocytosis prevents initiation of osteoclastogenesis but does not eliminate fusion with developing osteoclasts. *A* and *B*, Preosteoclasts were cytoplasmically labeled with PKH2 (green) or allowed to phagocytose PMMA particles and then labeled with PKH26 (red). The two cell populations were then cultured in the presence of 25 ng/ml M-CSF and 50 ng/ml RANKL either alone (*A*; original magnification ×50) or as cocultures (*B*; original magnification ×25). Equivalent results were obtained in three separate experiments. Osteoclasts formed exclusively from particle-free cells are indicated by arrows, and osteoclasts that have incorporated both particle-free and particle-containing cells are indicated with arrowheads. *C*, Preosteoclasts were cultured for 1 and 8 d with and without

PMMA particles (20 particles/cell) in medium supplemented with 25 ng/ml M-CSF. RNA was extracted and DC-STAMP and ATP6v0d2 expression measured by qPCR. DC-STAMP and ATP6v0d2 mRNA levels expressed relative to GAPDH were normalized to the day 1 samples without particles. $n = 5$. $*p < 0.05$ compared with equivalent sample without particles.

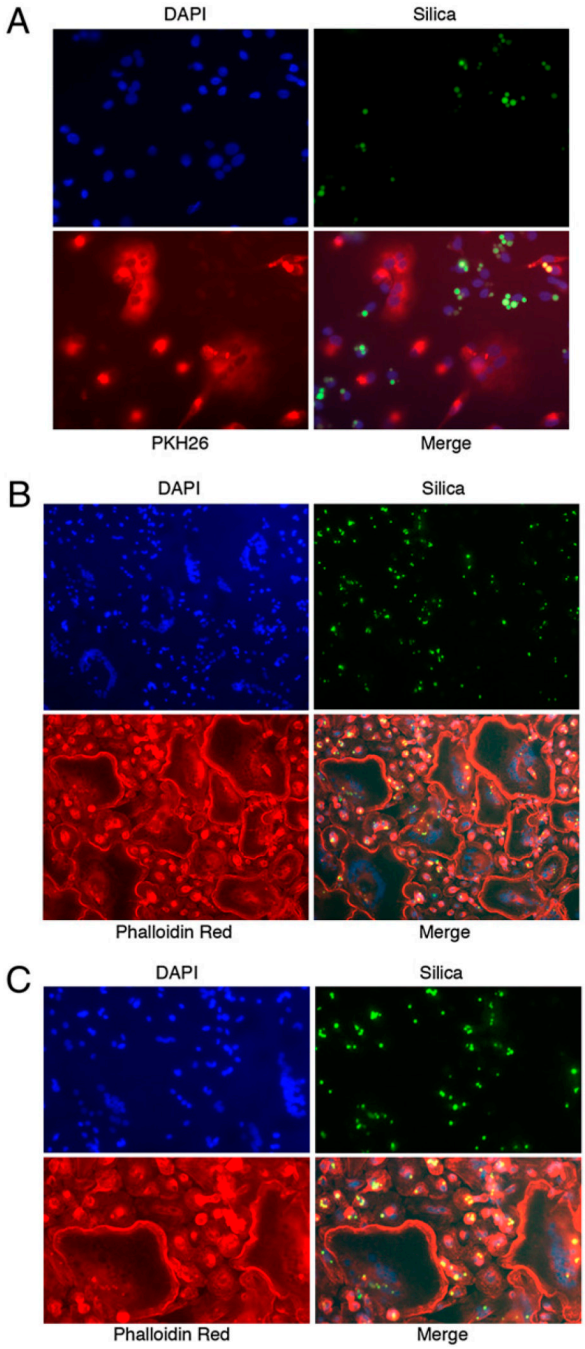

FIGURE 5.

Cells containing phagocytosed silica cannot initiate osteoclastogenesis, but may participate in cell fusion during later stages of osteoclast differentiation. Preosteoclasts were allowed to phagocytose green fluorescent silica particles and subsequently cocultured in the presence of 25 ng/ml M-CSF and 50 ng/ml RANKL with particle-free cells that had been labeled with PKH26 dye (*A*, red; original magnification ×50) or were unlabeled (*B*; original magnification ×25). Following culture, cells were labeled with phalloidin-Texas Red (*B*) and visualized by fluorescence microscopy. *C* shows a higher magnification (original magnification ×40) image of *B*. Equivalent results were obtained in two independent experiments.

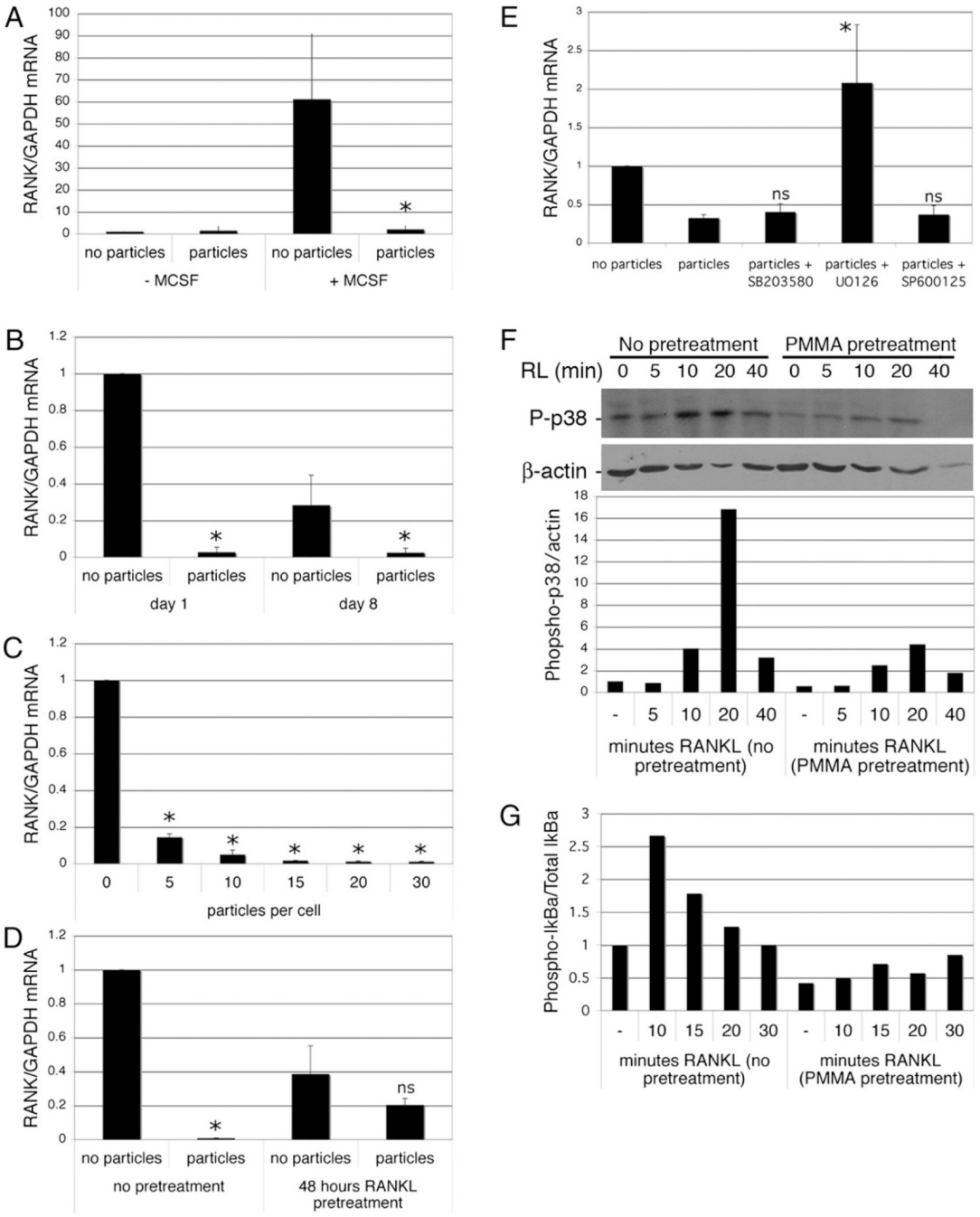

FIGURE 6.

Phagocytosis inhibits expression of RANK. *A*, Preosteoclasts were isolated and precultured overnight in the absence of M-CSF, then cultured with and without M-CSF (25 ng/ml) and PMMA (20 particles/cell). After 6 h, RNA was extracted and RANK expression measured by qPCR. RANK mRNA levels expressed relative to GAPDH were normalized to the cells treated without M-CSF or particles. $n = 3$. $^*p < 0.05$ compared with sample with M-CSF and without PMMA. *B*, Preosteoclasts were cultured for 1 and 8 d with and without PMMA particles (20 particles/cell) in medium supplemented with 25 ng/ml M-CSF. RNA was extracted and RANK expression measured by qPCR. RANK mRNA levels expressed relative to GAPDH were normalized to the day 1 samples without particles. $n = 5$. $^*p < 0.01$

compared with equivalent sample without particles. *C*, Dose dependency of particle-mediated repression of RANK expression in preosteoclasts 1 d after particle addition. $n = 3$. $^*p < 0.01$ compared with equivalent sample without particles. *D*, Preosteoclasts were cultured for 1 d with and without PMMA particles (20 particles/cell) in medium supplemented with 25 ng/ml M-CSF and 50 ng/ml RANKL with or without a 48-h pretreatment with RANKL. $n = 3$. $^*p < 0.01$ compared with equivalent sample without particles. *E*, Preosteoclasts were cultured for 6 h with and without PMMA particles (20 particles/cell) in medium supplemented with 25 ng/ml M-CSF. Where indicated, MAPK inhibitors were added 30 min prior to particles. RNA was extracted and RANK expression measured by qPCR. RANK mRNA levels expressed relative to GAPDH were normalized to the sample without particles. $n = 3$. $^*p < 0.05$ compared with sample with particles but no inhibitors. *F* and *G*, Preosteoclasts were incubated with or without particles for 24 h, after which they were challenged with RANKL. Protein extracts were prepared and analyzed by immunoblotting for phosphorylated p38 and actin (*F*) or phosphorylated IκBα and total IκBα (*G*). Quantitation (as described in *Materials and Methods*) was normalized to control (cells without RANKL or particles). Results from one of two similar experiments are shown.

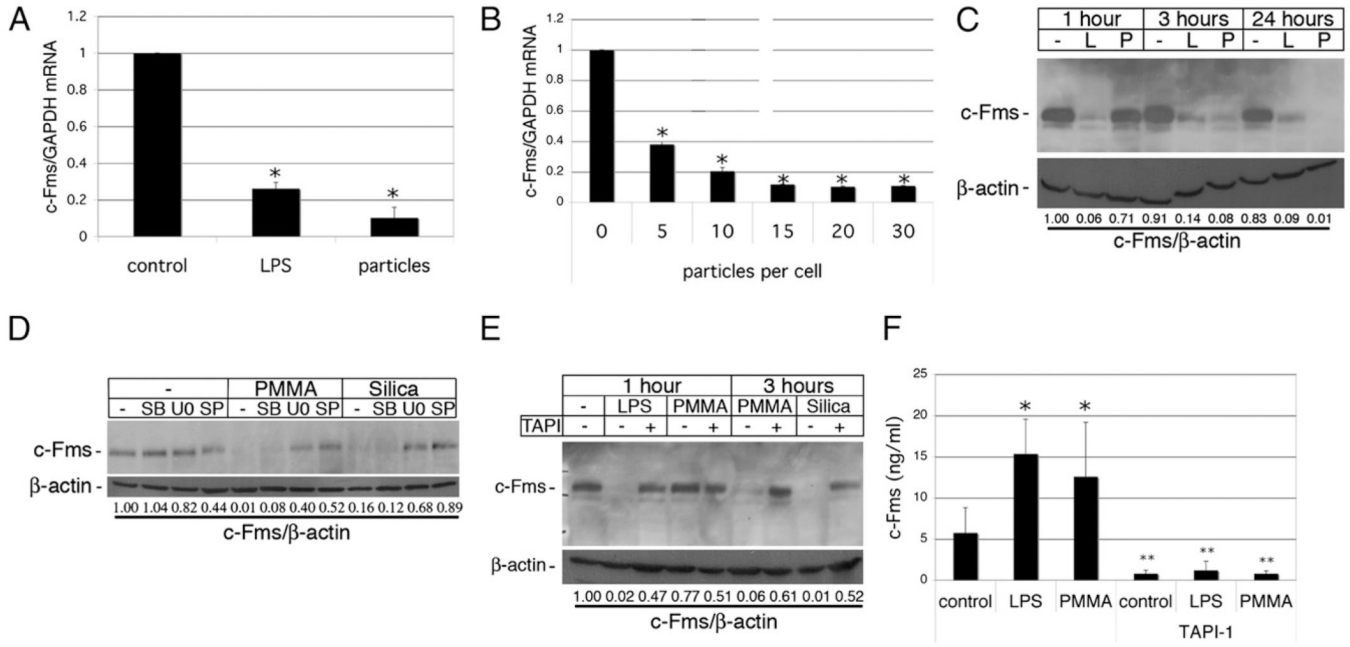

FIGURE 7.

Phagocytosis inhibits expression of c-Fms. *A*, Preosteoclasts were cultured for 1 d with and without PMMA (20 particles/cell) or 100 ng/ml LPS in medium supplemented with 25 ng/ml M-CSF. RNA was extracted and c-Fms expression measured by qPCR. c-Fms mRNA levels expressed relative to GAPDH were normalized to the control sample without particles or LPS. $n = 4$. $*p < 0.01$ compared with control. *B*, Dose dependency of particle-mediated repression of c-Fms expression in preosteoclasts 1 d after particle addition. $n = 3$. $*p < 0.01$ compared with equivalent sample without particles. *C*, Preosteoclasts were treated with PMMA or LPS for 1, 3, or 24 h, and whole-cell protein lysates were analyzed by immunoblotting with anti–c-Fms Ab. Membranes were then reblotted with anti–β-actin Abs, and c-Fms levels were quantitated relative to β-actin. *D*, Preosteoclasts were preincubated with the MAPK inhibitors SB203580 (SB), U0216 (U0), and SP600125 (SP) for 30 min prior to addition of PMMA or silica (20 particles/cell). After 3 h, protein extracts were prepared and analyzed by immunoblotting as above. *E*, Preosteoclasts were pretreated with TAPI for 30 min prior to addition of LPS or particles. After 1 or 3 h, protein extracts were prepared and analyzed by immunoblotting. *F*, Preosteoclasts were pretreated with TAPI for 30 min and then treated with or without PMMA or LPS for 3 h, and c-Fms ectodomain shed into conditioned media was analyzed by ELISA. $n = 3$. $*p < 0.01$ compared with control; $**p < 0.01$ compared with equivalent samples without TAPI.